Numerical modeling and physical properties of magma

Résumé français du chapitre (II)

Dans cette partie de la thèse, nous essayons d'expliquer brièvement les paramètres physiques du magma qui jouent un rôle important pour le transfert de chaleur et l'écoulement de fluide. Puis nous décrivons la construction du modèle et nous terminons avec la validation de notre modèle avant les applications.

1. Paramètres physiques

L'évolution de la distribution de la température en n'importe quelle structure est régie par les propriétés thermiques du matériel, en particulier par la capacité calorifique et la conductivité thermique.

1.1 Conductivité thermique

C'est la propriété d'un matériel qui indique sa capacité à transférer la chaleur de façon conductive. La conductivité thermique ($W.m^{-1}.K^{-1}$) varie inversement avec la température. Ainsi des mesures de conductivité thermique en fonction de la température montrent généralement que la conductivité thermique diminue avec l'augmentation de température, jusqu'environ à 1000-1200°C (Clauser, 1988). Les équations suivantes expriment la conductivité thermique en fonction de la température pour les roches magmatiques, métamorphiques, sédimentaires et l'eau :

$$\lambda_{\text{roches magmatiques}} = -0.0016(T) + 2.6842 \quad \text{(II.1)}$$

$$\lambda_{\text{roches métamorphiques}} = -0.0023(T) + 3.1138 \quad \text{(II.2)}$$

$$\lambda_{\text{roches sédimentaires}} = -0.0044(T) + 4.0276 \quad \text{(II.3)}$$

$$\lambda_{\text{l'eau}} = 0.0012(T) + 0.2557 \quad \text{(II.4)}$$

où T est la température en K.

1.2 La capacité calorifique

Également connu en tant que *chaleur spécifique*, c'est la quantité de chaleur qu'il faut fournir à un système pour élever sa température d'un kelvin. Dans le Système International d'unités, la capacité calorifique s'exprime en joules par kelvin ($J.K^{-1}$). Comme nous avons fait pour la conductivité thermique, nous essayons de trouver un rapport mathématique simple expriment la relation entre la capacité calorifique et la température:

$$C_{P\ \text{roches magmatiques}} = 0.6169(T) + 626.32 \quad \text{(II.5)}$$

$$C_{P\ \text{roches métamorphiques}} = 0.5915(T) + 636.14 \quad \text{(II.6)}$$

$$C_{P\ \text{roches sédimentaires}} = 0.5814(T) + 683.07 \quad \text{(II.7)}$$

$$C_{P\ \text{l'eau}} = 16.782(T) + 2013.2 \quad \text{(II.8)}$$

1.3 Densité

Elle est définie comme le quotient de la masse *m* et du volume v d'un matériel. ($\rho = m*v^{-1}$), l'unité de SI pour la densité est $kg \cdot m^{-3}$. La densité de n'importe quel matériel change avec la température. La diminution de la densité avec la température jusqu'à 1000°C est entre 11- 13 %.

L'équation qui exprime la variation de densité par rapport aux changements de température pour obtenir la convection thermique est:

$$\rho = \rho_0 \left(1 - a_v \left(T - T_0\right)\right) \quad \text{(II.9)}$$

Où ρ est la densité à T_0 et α_v est le coefficient volumétrique de dilatation thermique.

1.4 Viscosité

Elle mesure de la facilité de l'écoulement d'un liquide et de la mobilité des ions; elle représente une mesure de la résistance à l'écoulement. Une relation mathématique qui exprime la relation entre la viscosité et la température est nécessaire pour la simulation numérique qui étudie la mise en place de magma et la circulation hydrothermale. Le rapport entre la viscosité et la température peut être exprimé par une équation d'Arrhénius :

$$\mu = C * e^{\left(Ea/RT\right)} \quad \text{(II.10)}$$

où μ est la viscosité, C c'est une constante, Ea est l'énergie d'activation, égale à 30 $K*J*mole^{-1}$ et R la constante de gaz universelle, égale à 8.314472 $J*K^{-1}*mol^{-1}$.

1.5 La perméabilité et la pression du fluide

La perméabilité est la capacité d'un matériel à transmettre le fluide; l'unité SI pour la perméabilité est en mètres carrés; ce paramètre est un paramètre géologique critique car la migration de fluides joue un rôle fondamental dans le processus de minéralisation.

Ingebritsen et Manning, (2003) ont proposé un rapport exponentiel entre la perméabilité et la profondeur, basé sur des études et des évaluations géothermiques de flux de fluide métamorphique:

$$Log\left(K\right) \approx -14 - 3.2 \log\left(z\right) \quad \text{(II.11)}$$

où K est la perméabilité et le z est la profondeur (km).

La pression du fluide peut réduire la force de roche et provoquer une rupture fragile par la tension efficace principale en profondeur (z). Donc, la pression du fluide par rapport à la tension verticale s'exprime par l'équation suivante:

$$\sigma_v' = (\sigma_v - P_f) = \rho_R g z (1 - \lambda_v) \quad \text{(II.12)}$$

où le σ_v est la pression efficace, P_f la pression du fluide, ρ_R la densité de la roche, z la profondeur, g l'accélération de la gravité et λ_v est le facteur de fluide de pore.

Pour estimer l'influence de l'advection thermique, nous avons utilisé le nombre de Péclet qui décrit le rapport entre l'advection et la diffusion thermique. Le nombre de Péclet est un nombre sans dimensions de la vitesse moyenne de l'écoulement et permet de comparer l'advection à la diffusion. On le lie aux paramètres sans dimensions Re (le nombre de Reynolds) et Pr (nombre de Prandtl), Le nombre de Péclet peut être écrit comme:

$$\mathrm{Pe} = u\, R / \underline{\kappa} \quad \text{(II.13)}$$

Où u est le vecteur de vitesse du fluide, R est la dimension caractéristique de l'objet étudié en (m) et $\underline{\kappa}$ est la diffusivité thermique.

2. La construction du modèle

L'équation principale qui calcule la température dans la partie thermique de nos modèles (et qui inclut le transfert de chaleur par de convection et conduction) est exprimée comme:

$$S.C_{eq}\left(\frac{\partial T}{\partial t}\right) + \nabla\left[-\lambda_{eq}\nabla T + C_L \vec{u} T\right] = Q \quad \text{(II.14)}$$

Où S est le terme de stockage, C_{eq} dénote la capacité de chaleur volumétrique efficace ; le λ_{eq} définit la conductivité thermique efficace ; et le C_L est la capacité de chaleur volumétrique du fluide mobile. Le côté droit de l'équation (Q) correspond à la source de chaleur générale.

Quand ce qui contrôle le mouvement de fluide dans le milieu poreux est le gradient de potentiel hydraulique, la loi de Darcy s'applique. Selon cette loi, le flux net qui traverse une surface poreuse est :

$$u = -K/\mu\,(\nabla P + \rho_f g \nabla z) \quad \text{(II.15)}$$

Où u est la vitesse de Darcy, K est la perméabilité du milieu poreux, μ est la viscosité dynamique du fluide.

La continuité de la loi de Darcy est exprimée par:

$$\partial P / \partial t + \nabla.\left[-K/\mu(\nabla P + \rho_f g \nabla z)\right] = Q_s \quad \text{(II.16)}$$

Où S est le terme de stockage,

Les modèles ont été divisés en deux types : un type de modèles théoriques où nous avons simulé les modèles hypothétiques pour examiner les effets de la profondeur de la mise en place, de la forme de pluton ou des zones perméables. Il a été également inclus dans cette partie la simulation de différents exemples, tous étant faits en 2D. Le deuxième type de modèles a été construit pour simuler un exemple particulier venant du Maroc Central avec une géométrie plus compliquée et plus réaliste du pluton; cette partie a été faite en 3D.

Enfin la validation de nos modèles a été réalisée pour simuler deux modèles publiés (Rabinowicz et al 1998, et modèles de Gerdes et al., 1998) et pour comparer l'observation de terrain de certains exemples normaux avec nos modèles numériques équivalents (pour plus de détails voir ci-dessous).

1. The code:

COMSOL is a general purpose reactive-transport code developed for a variety of scientific problems, thermal and earth sciences problems are one of them. Simulations can be solved for coupled fluid flow, heat transfer and water-rock interactions, as well as the ability to solve these functions individually. To solve the PDEs (partial differential equations), COMSOL Multiphysics uses the *finite element method (FEM)*. For example a PDE will involve a function u(**x**) defined for all **x** in the domain with respect to some given boundary condition. The purpose of the method is to determine the function u(**x**). The method requires the discretisation of the domain into subregions or cells. For example a two-dimensional domain can be divided by a set of triangles (the cells). On each cell the function is approximated by a characteristic form. For example u(**x**) can be determined by a linear function on each triangle. The software runs the finite element analysis together with adaptive meshing and error control using a variety of numerical solvers.

In numerical modeling, the discretization of the model into small subdomains (primitives hexahedra and tetrahedra in 3D and quadrilaterals and triangles in 2D) is fundamental to facilitate the calculation. The governing equations are then solved inside each of these subdomains, with an assurance to keep the continuity of solution across the common interfaces between two subdomains. So, the solution inside each portion can be a part of the main picture of fluid flow in the entire model. Those subdomains are called cells, and all elements or cells together are called a mesh or grid. The process of obtaining an appropriate mesh (or grid) is termed mesh generation (or grid generation).

Comsol multiphysics was made to solve different physical problems such as heat transfer, electromagnetics, fluids dynamics, structural mechanics and others, in addition to earth sciences. It was used to valid or study different phenomena. Comsol-multiphysics is upgraded frequently and its validation is carried out each year by an international conferences and published papers which are made especially for Comsol-Multiphysics applications.

2. Parameters and free convection mode

Fluids are produced in the earth's crust by different mechanisms such as devolatilization reactions (organic matter, H_2O and CO_2 during diagenesis and metamorphism) and fluid release during crystallisation of magmas. However, infiltration of meteoric waters and migration of fluids between distinct reservoirs can disturb these initial fluid compositions and temperatures by mixing processes. Fluid flows are driven by several driving mechanisms, including: (1) Topography- or gravity driven flow; (2) compaction-driven flow during basin subsidence; (3) seismic pumping and tectonically driven flow; and (4) buoyancy driven flow

(Kühn et al., 2006). Migration of fluids outside their initial reservoir and/or production zone results necessarily in fluid mixing. This process is especially developed in environments where fluid circulation is active such as sea floor hot springs and numerous geothermal systems (e.g. Fournier, 1977; Fournier, 1973; Dubois et al., 1994). The conclusion of Gessner et al. (2006) suggests that thermally driven flow or free convection is one possible mechanism.

2.1 Physical Parameters

The basic mechanism for heat transport is heat conduction. Heat conduction responds to gradients of temperature. However, additional heat transfer will also be accomplished by advection due to the movement of the three phases: solid, liquid and gas. The latent heat inherent to phase changes may also have significant thermal effects. The evolution of the temperature distribution in any structure is governed by the thermal properties of the material, particularly heat capacity and heat conductivity. In the case of intruded magma, it is hard to determine these properties because of the numerous phenomena that occur simultaneously within the magma, and they can not be separated easily. These effects include in particular the evolution of the porosity, water content, type and amount of crystallization, changes in the chemical composition (Vosteen et al., 2003). Therefore, in this section, we will try to illustrate the thermal properties.

2.1.1 Thermal Conductivity (λ)

Thermal conductivity as a function of high temperature is isotropic for many volcanic and plutonic rocks; in contrast, thermal conductivity of some sedimentary and many metamorphic rocks may be strongly anisotropic and difficult to measure due to the influence of many petrophysical parameters such as the evolution of the porosity and moisture content (in sediments and volcanic rocks), the dominant mineral phase (in metamorphic and plutonic rocks), and the anisotropy (in sediments and metamorphic rocks) (Clauser and Huenges, 1995).

2.1.1.1 The influence of porosity and the dominant mineral phase

Clauser and Huenges (1995), provided experimental evidence to prove that thermal conductivity varies inversely with porosity, this role is applicable for volcanic rocks, high porosity distribution is clearly skewed towards low conductivities.

Because plutonic and metamorphic rocks display a much smaller and similar porosity, the dominant mineral phase controls different conductivity distributions. For plutonic rocks, the feldspar content is the main mineral dominant, therefore high feldspar content (more than 60%) biases the distribution towards low conductivities. In contrast to that, quartz content presents the dominant mineral phase in metamorphic rocks, low conductivity part is made up of rocks with low quartz content; the high conductivity portion consists of quartzite only.

2.1.1.2 The influence of surrounding temperature

The thermal conductivity reduction due to the temperature is marked clearly for materials except some amorphous or fused materials such as obsidian but they aren't discussed here. Thermal conductivity varies inversely with temperature, thus measurements of thermal conductivity as function of increasing temperature generally show initially a decrease with temperature, until around 1000-1200 °C (Clauser, 1988). Volcanic glasses and rocks with a small iron content increase in thermal conductivity for temperatures above 800-1000°C. Above around 900°C, the decrease of thermal conductivity with temperature is quite different, depending on the feldspar content: while there is no significant decrease (roughly 10%) in conductivity up to 300°C for rocks that are rich in feldspar, rocks that are poor in feldspar decrease by more than 40%. For metamorphic rocks, the decrease of thermal conductivity with temperature depends on the content in a dominant mineral phase. In rocks poor in quartz the decrease in conductivity amounting to about one third of the room temperature value up to 200°C, then it remains roughly constant up to 500°C (Clauser, 1988; Clauser and Huenges, 1995; Vosteen and Schellschmidt, 2003).

In our numerical modelling, detailed search was made to obtain experimental data available in the literature; often data on thermal conductivity is available for room temperature conditions only. Therefore some empirical relationships have been proposed for extrapolation on the basis of data measured at quite elevated temperature. Figure (II.1a,b and c) gives one of these databases for thermal conductivities (Vosteen and Schellschmidt, 2003). The thermal conductivity was varied with temperature by using the following linear relations:

$$\lambda_{\text{magmatic rocks}} = -0.0016(T) + 2.6842 \quad \text{(II.1)}$$

$$\lambda_{\text{metamorphic rocks}} = -0.0023(T) + 3.1138 \quad \text{(II.2)}$$

$$\lambda_{\text{sedimentary rocks}} = -0.0044(T) + 4.0276 \quad \text{(II.3)}$$

$$\lambda_{\text{water}} = 0.0012(T) + 0.2557 \quad \text{(II.4)}$$

Where λ is thermal conductivity in ($W.m^{-1}.K^{-1}$) and T is temperature in K.

The expressed property equations developed in this work are theoretically derived from empirical data. To simplify the experimental data we assumed that the relation between the thermal conductivity and temperature is always linear, and the effects of the water and gas content and porosity are negligible.

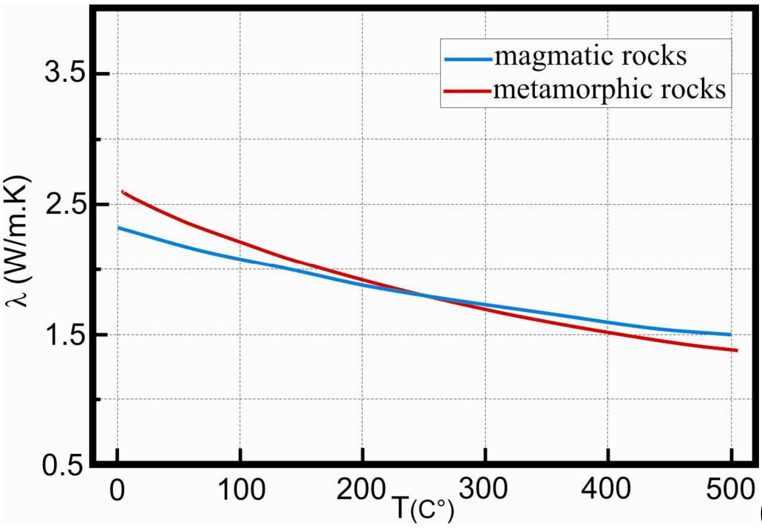

(a)

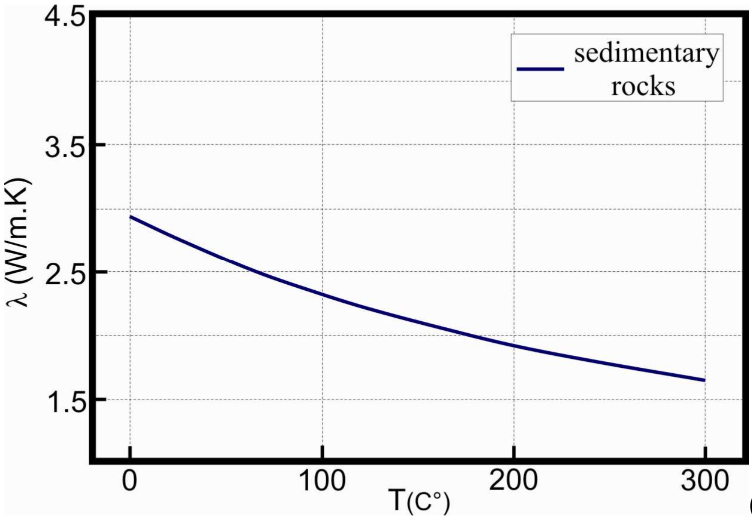

(b)

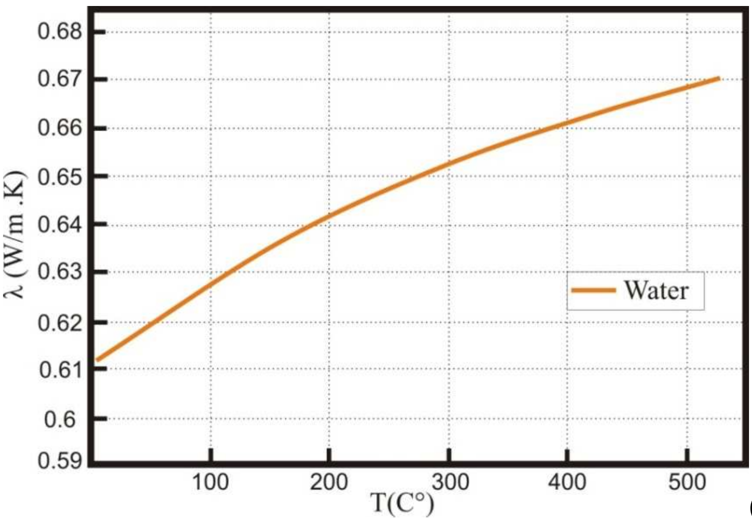

(c)

Figure (II.1): Thermal conductivity of water and different types of rocks, a) for magmatic and metamorphic rocks, b) for sedimentary rocks, c) for water (modified after Vosteen and Schellschmidt 2003).

Based on the previous lecture survey, this simplification is acceptable because the maximum temperature applied in our models was 700 C°, for this thermal limit, the assumption of linear relationship between temperature and thermal conductivity is likely acceptable.

2.1.2 Specific Heat Capacity (c_P)

It is notice that the measurements of specific heat capacity on rock materials are more rarely than thermal conductivity. Nevertheless, heat capacity ($J.kg^{-1}.K^{-1}$) is defined as the amount of heat required to raise the temperature of the unit mass (1 kg) of a substance by a unit temperature increase (1 K). The heat capacity designated by c_p, may be expressed as follows (Schaërli & Rybach, 2000):

$$c_p = \left(\frac{\partial H}{\partial T}\right)_p \tag{II.5}$$

Where H is enthalpy (in J).

Specific heat capacity is fundamentally important in geothermal calculations because its value is reated to the amount of material in the object, the thermal conductivity λ ($W.m^{-1}.K^{-1}$) and the thermal diffusivity κ ($m^2.s^{-1}$) by the equation:

$$\kappa = \left(\frac{\lambda}{C_p * \rho}\right) \tag{II.6}$$

where ρ is density $kg.m^{-3}$.

Values for the specific heat capacity of gases, fluids and solid materials such as metals, some rocks or other substances are reported in the literature. The specific heat of gases and fluids plays a role in porous rocks. In most cases the pore filling is water, and sometimes air, oil or mixtures of the three. A large number of data on specific heat capacities of elements and rocks or minerals are reported by Vosteen and Schellschmidt (2003).

As we have done for the thermal conductivity, we attempt to find a simple mathematic relationship expressing the relation between specific heat capacity and temperature based on literature data. Figure (II.2a, and b) summarize the empirical results done by Vosteen and Schellschmidt (2003).

The following linear relationships show the temperature-dependance laws for heat capacity of different type of rocks and water:

$$c_{P\ \text{magmatic rocks}} = 0.6169(T) + 626.32 \tag{II.7}$$

$$c_{P\ \text{metamorphic rocks}} = 0.5915(T) + 636.14 \tag{II.8}$$

$$c_{P\ \text{sedimentary rocks}} = 0.5814(T) + 683.07 \tag{II.9}$$

$$c_{P\ \text{water}} = 16.782(T) + 2013.2 \tag{II.10}$$

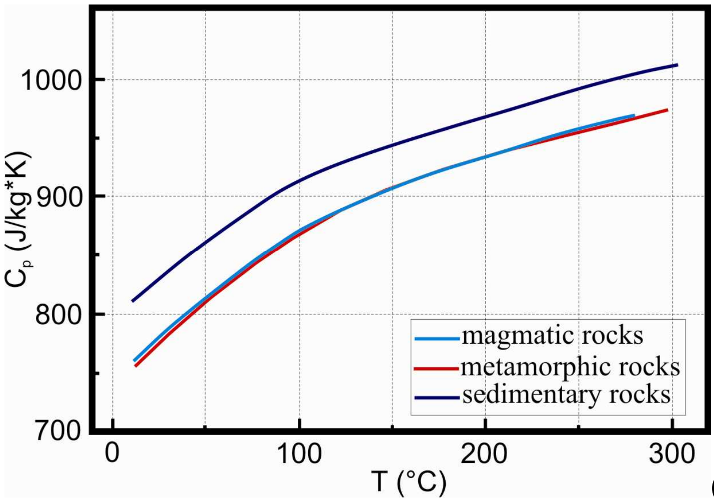

(a)

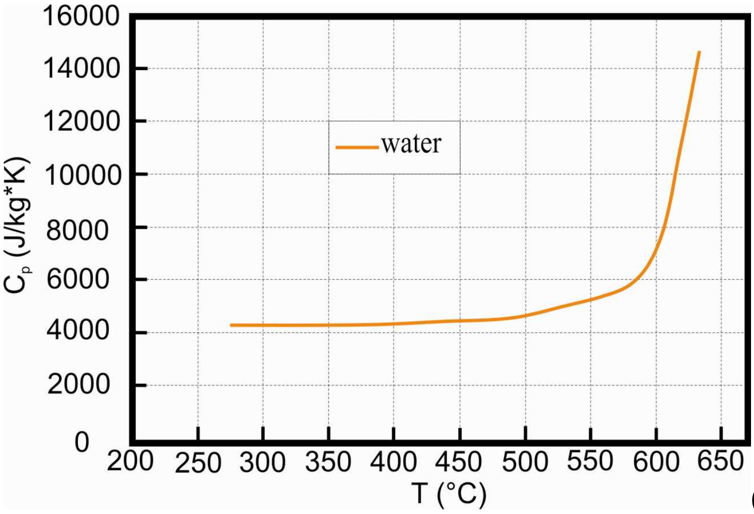

(b)

Figure (II.2): Specific heat capacity varies with temperature for a) magmatic, metamorphic, sedimentary rocks, b) and water (modified Vosteen and Schellschmidt 2003).

2.1.3 Density

Density (ρ) is defined as the quotient of the mass *m* and the volume V of a material. $\rho = m.v^{-1}$. The SI unit for density is $kg{\cdot}m^{-3}$. The density of any material changes with temperature. The relative decreasing of density with temperature up to 1000°C is between 11-13 %. When a fluid or rock is heated, its density generally decreases (for rock too especially when we deal with the geological time scale) because of thermal expansion.

Figure (II.3) shows that fluids heated from below or within become gravitationally unstable, because the cold part tends to sink while the hot part rises. This phenomenon called thermal convection (Turcotte and Schubert, 2002).

Chemical composition and specially water included are important parameters affecting on the density of liquids such as melts. Figure (II.4) shows that the variation of density based on chemical composition could be small or large over a range of several hundreds of degrees

Celsius, such as between melts of contrasting major-element composition (between basalt and rhyolite) (Best, 2001).

The thermal convection that driven by buoyancy forces is essentially depends on density variations. To take into account the buoyancy forces, we must take into our account small density variations in vertical force balance:

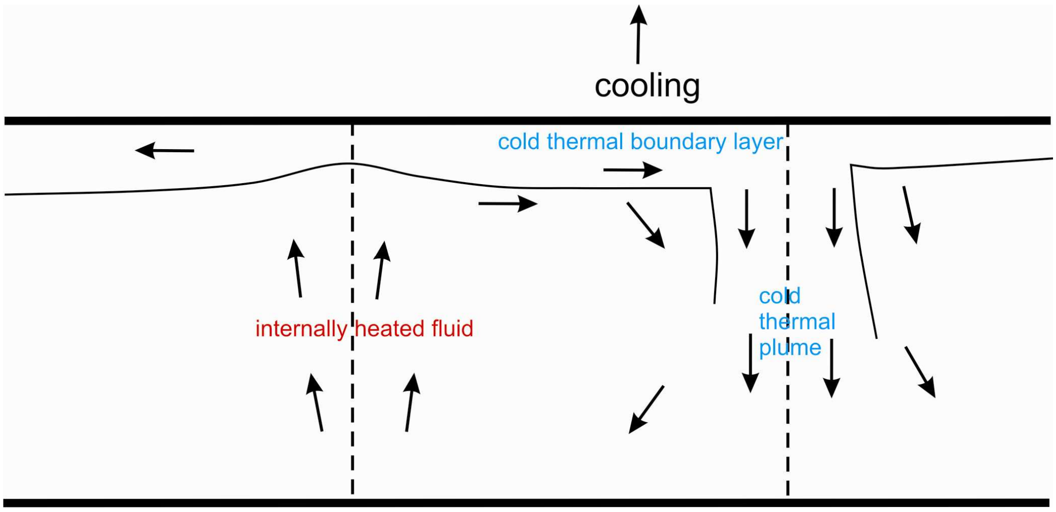

Figure (II.3): The idea of thermal convection in a fluid layer heated from within and cooled from above. (modified after Turcotte and Schubert, 2002).

$$\rho = \rho_0 + \rho' \qquad \text{(II.11)}$$

Where ρ_0 is a reference density and ρ' is a density varied with temperature.

Specific densities at constant P and T can be calculated at another P and T by using compressibility and thermal expansion data for rocks and melts (Lange & Baker, 2001).

The coefficient of isothermal compressibility β, expresses the change in volume or density as P changes with depth in the earth at constant T:

$$\beta = -\left(\frac{1}{V}\right)\left(\frac{dV}{dP}\right)_T = -\left(\frac{1}{\rho}\right)\left(\frac{d\rho}{dP}\right)_T \qquad \text{(II.12)}$$

Where V is the molar volume.

Because dV/dP is negative β is positive; it has units of reciprocal pressure. For crystalline solids (Lange & Baker, 2001), $\beta = 1\text{-}2 * 10^{-11}\ Pa^{-1}$, for melts, $\beta \sim 7*10^{-11}\ Pa^{-1}$ and water 1.7 Pa^{-1}. The volumetric coefficient of thermal expansion α_v, expresses the change in volume or density as T changes at constant P.

$$a_v = -\left(\frac{1}{V}\right)\left(\frac{dV}{dT}\right)_P = -\left(\frac{1}{\rho}\right)\left(\frac{d\rho}{dT}\right)_P \qquad \text{(II.13)}$$

α_v has units of reciprocal degrees. Most minerals and rocks have a thermal expansion in the range of $1\text{-}5*10^{-5}\ deg^{-1}$, for many silicate melts, $\alpha_v \sim 3*10^{-5}\ deg^{-1}$ and for water $4.7*10^{-4}\ deg^{-1}$.

The densities of natural melts depend mostly on their chemical composition; especially the concentration of water and its changes during crystallization is more dramatic.

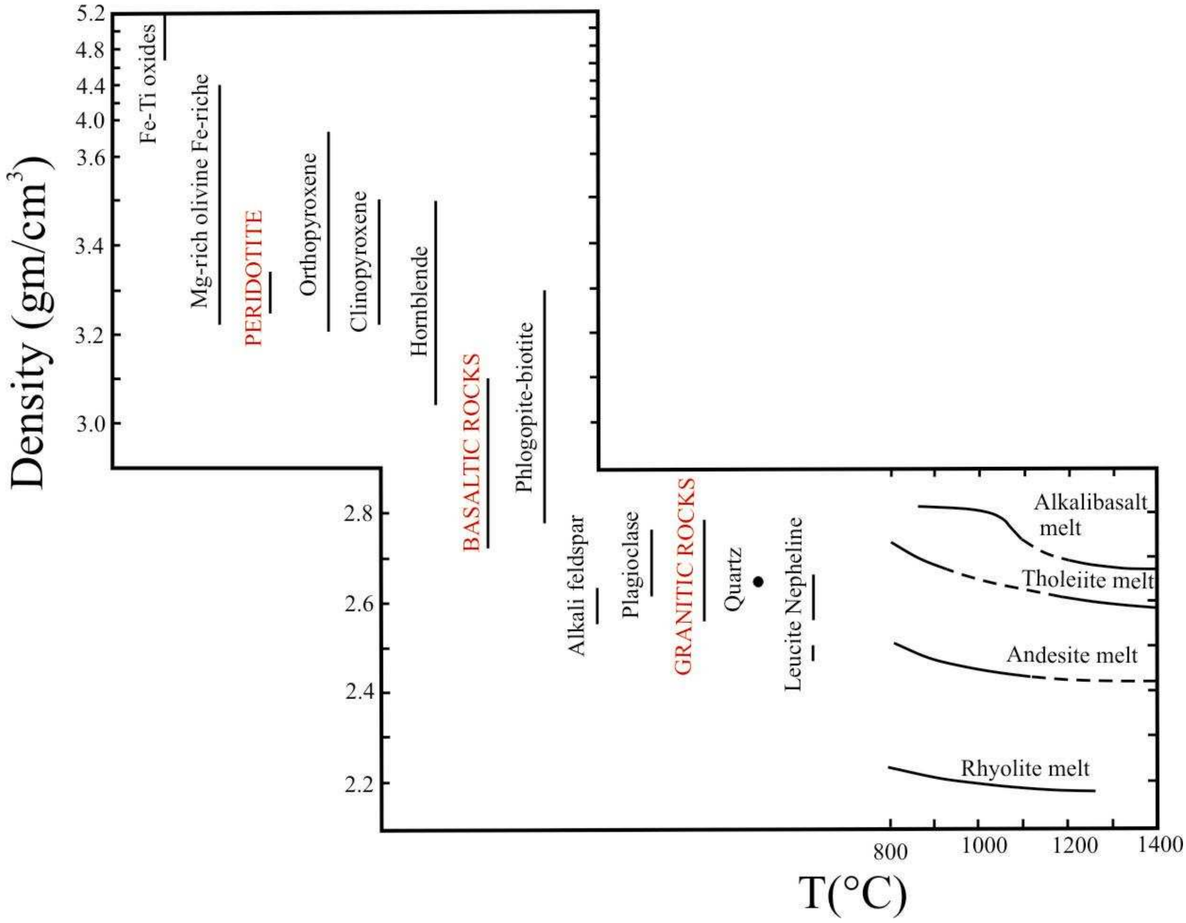

Figure (II.4): Densities of common rock-forming minerals and rocks at atmospheric P and T and melts at 1 atm. Higher densities for mafic solid-solution silicates are Fe-rich end members; lower densities are Mg-rich end members. Note change in density scale in upper left. Experimentally measured densities for crystal-free melts. (modified after Murase and McBirney, 1973).

For example, dissolving only 0.4 wt.% water in a basalt melt at 1200°C and 700 bars has the same effect on density as increasing T by 175°C or decreasing P by 2300 bars (Ochs and Lange, 1997). Following to our simplification, we once again introduce a relation between temperature and density to create thermal convection as we consider the variation of density with pressure is small and then negligible. The density variations caused by temperature changes are given by Turcotte and Schubert (2002):

$$\rho' = -\rho_0 a_v (T - T_0) \tag{II.14}$$

By substitution of equation [II.13] into equation [II.10], we obtain:

$$\rho = \rho_0 (1 - a_v (T - T_0)) \tag{II.15}$$

Equation [II.15] is our expression for density variation with temperature changes, to create and obtain thermal convection.

2.1.4 Viscosity

Viscosity is a measure of the ease of flow of a melt and the mobility of ions, or is a measure of the resistance to flow. Thus, viscosity is a manifestation of mobility. In other words, fluidity is the term used to express the contrast of viscosity.

The unit of viscosity is the Pa s (Pascal*second) or the poise (10 poise = Pa s). Viscosity is the most important property of melts that controls the dynamic behaviour of magmas. Segregation of partial melts in upper mantle and lower crustal sources, magma ascent to shallower depths, intrusion, extrusion as lavas or as explosive fragments, and crystallization all depend on the viscosity of the melt. To demonstrate the importance of viscosity in the mobility of fluids, we take the tar (asphalt) as an example. Tar at 24°C is more viscous than honey, which is more viscous than water. One principal factor governing viscosity of fluids is their temperature. For any melt or fluid composition, higher T reduces the viscosity by losing the melt or fluid structure through the increased kinetic energy of the atoms; ionic mobility is enhanced. Figure (II.5) illustrates the strong dependence of melt viscosity on T and composition. (Best, 2003). For example, the dependence on T is shown by the fact that between 700°C and 1000°C the viscosity of a water-free rhyolite melt decreases by six orders of magnitude, from about 10^{15} to 10^{9} Pa s (Murase and McBirney, 1973; Webb and Dingwell, 1990; Dawson et al., 1990).

Briefly, based on the previous paragraphs, a mathematic relation expresses the relation between viscosity and temperature is necessary to be accounted for in the numerical simulation which studies the hydrothermal coupling pre—syn and post-magma emplacement. Based on Turcotte and Schubert (2002), viscosity dependence temperature can be expressed by Arrhenius equation:

$$\mu = C * e^{\left(Ea / RT \right)} \tag{II.16}$$

Where μ is viscosity, C is a constant, Ea is activation energy, equal to 30 K*J/mole and R is universal gas constant, equal to 8.314472 J/K*mol.

This equation is applicable for both melts and fluids because both of them have a Newtonian behaviour. Where Newtonian fluid is a fluid behaves like water-its shear stress is given by:

$$\tau = \mu * \left(\frac{\partial u}{\partial x} \right)$$

Where τ is the shear stress exerted by the fluid, μ is the fluid viscosity and ∂u/∂x is the velocity gradient perpendicular to the direction of shear.

The viscosity of a Newtonian fluid is the constant of proportionality between shear stress and strain rate. The constant C can be eliminated by referencing the viscosity to its value at the upper boundary μ_0, the variation of viscosity of water with temperature then can be determined by the following equation (Kestin et al., 1978):

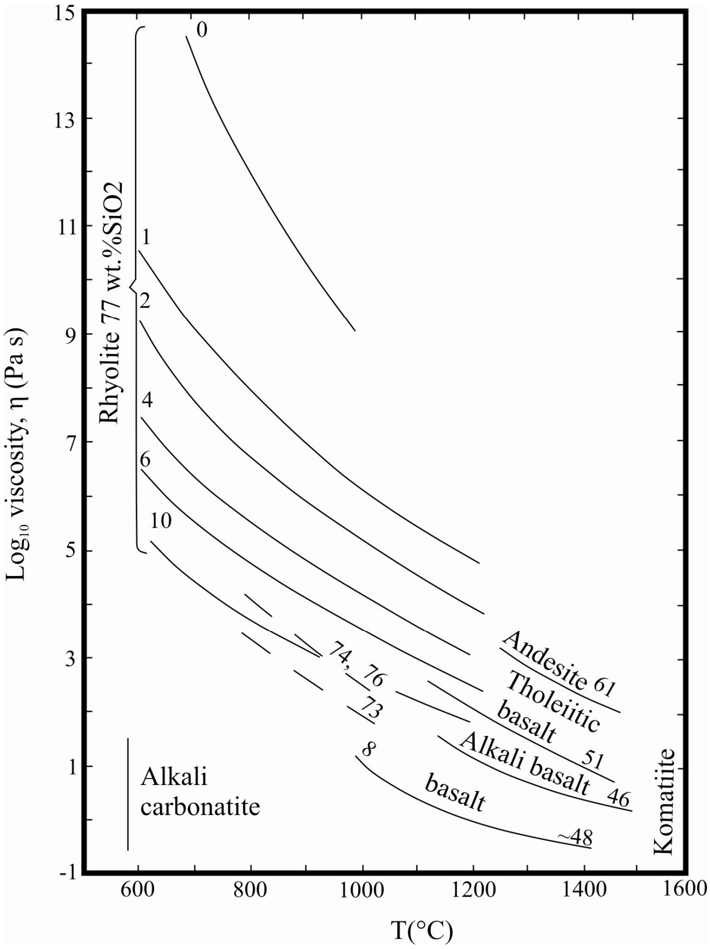

Figure(II.5): Newtonian viscosities of some crystal and melts as a function of T at 1 atm. P dependences are negligible. Concentrations of silica in weight percentage are indicated as well as of water in weight percentage at low-T end of curves, (modified after Murase and McBirney, 1973).

$$\mu = 2.414 * 10^{-5} * 10^{\left(\frac{247.8}{(T+133)}\right)} \quad \text{II.17)}$$

2.1.5 Permeability and fluid pressure

Permeability is the capacity of a material to transmit fluid, the SI unit for permeability is square meter; it is a critical geological parameter because migrating fluids play a fundamental subsurface role in ore deposition, hydrocarbon maturation and migration, seismicity, and metamorphism.

The majority of significant ore deposits exist because of the advective solutes and heat by fluid circulation, transport, and deposition of chemical species are all linked to fluid flow, and the thermal effects of fluid flow can explain the emplacement of certain types of ore deposits (Ingebritsen and Manning, 1999). Numerical modelling in different geological environments shows that permeability is the most important factor in fluid flow which occurs throughout the continental crust, from the surface to at least 15km depth (Famin et al., 2004). However, it is difficult to determine exactly a relation for permeability related depth, because the permeability is varying with time by different processes such as dissolution-precipitation reactions, compaction, fracturing and poroelastic response. For this reason, we can say that permeability is a parameter that depends on depth and time, which means, the permeability's value changes with different depths at fixed time and it is also varying with time at constant depth, especially when we deal with long time intervals like geological time periods. To simplify our models, we assumed that permeability is constant with time and varies only with depth. Another problem makes the mathematic expression of permeability related depth more difficult is that at the zone of brittle-ductile transitional zone, permeability decreases and varies strongly (Ingebritsen and Manning, 2003 ; Famin et al., 2004).

However, Ingebritsen and Manning (2003) proposed based on geothermal studies and estimates of metamorphic fluid flux a quasi-exponential decay of permeability (K in m²) with depth (z in km) of:

$$Log\left(K\right) \approx -14 - 3.2\log\left(z\right) \tag{II.18}$$

Figure (II.6) shows permeability as function of depth in continental crust, based on geothermal and metamorphic data. This equation was used in our models to vary permeability with depth starting from 100m as we consider the upper 100m of the crust represented by quaternary deposits.

Fluid pressure may reduce rock strength and causes brittle failure through the principle of effective stress, at depth (z); it is convenient to defined fluid pressure with reference to vertical stress (overburden pressure) by

$$\sigma_v' = \left(\sigma_v - P_f\right) = \rho_R g z \left(1 - \lambda_v\right) \tag{II.19}$$

Where σ_v' is effective overburden pressure, σ_v overburden pressure, P_f is fluid pressure, ρ_R is rock density, z is depth, g is gravitational acceleration and λ_v is pore fluid factor.

Pore fluid factor is the variable which controls which type of fluid pressure dominates with depth, and we can calculate it by using the following equation:

$$\lambda_v = \rho_w / \rho_R \tag{II.20}$$

Where ρ_W is water density.

Fluid overpressuring may arise through the following: 1) compaction, especially in areas of rapid sedimentation; 2) diagenetic and metamorphic dehydration processes aided by organic maturation; 3) igneous intrusion into fluid saturated crust; and perhaps 4) direct linkage to zones of mantle degassing, as recently postulated for San Andreas Fault system (Sibson, 2001).

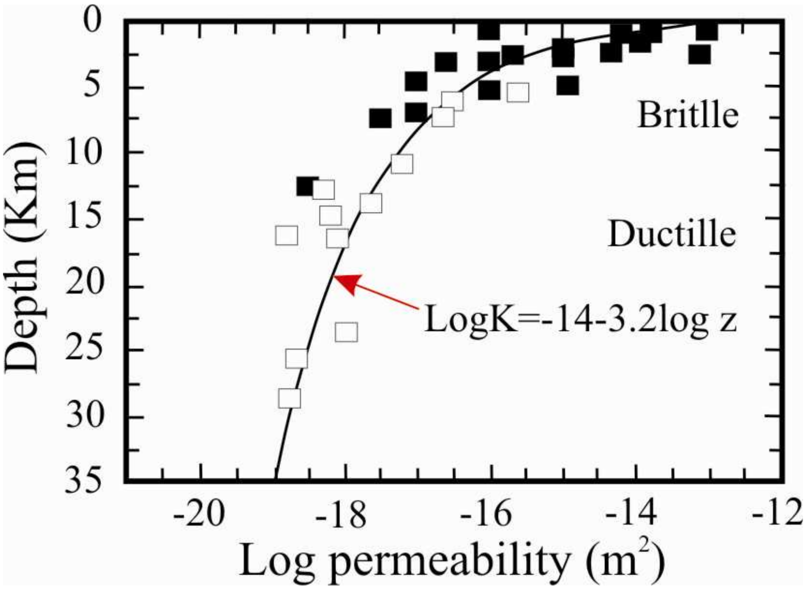

Figure (II.6): Permeability related depth curve based on geothermal data (solid squares), and metamorphic systems (open squares), (modified after Ingebritsen and Manning, 2003).

At few kilometres depth, fluid pressure is abutting to hydrostatic values (with $\lambda_v < 0.4$), with increasing depth to be more than several kilometers λ_v's values exceed hydrostatic pressure and being adjacent to lithostatic values ($\lambda_v \rightarrow 1.0$); fluid pressure levels are assumed to be near-lithostatic pressure ($\lambda_v \approx 1.0$ with $P_f \approx \sigma_v$) where the prograde metamorphism is dominated figure (II.7), (Etheridge et al., 1984; Sibson, 2001).

2.2 Free convection theory

A porous medium heated from below has an unstable situation, because cool fluid tends to sink and hot fluid tends to rise. This situation leads to free thermal convection as soon as viscous forces are not too high (Kühn et al., 2006).

On the one hand, Rayleigh convection occurs when Rayleigh number (non dimensional number representing the ratio between driving and resisting forces to fluid flow), exceeds a critical value (Eq. (II.21) & Figure (II.8)). If the thermal gradient (or any of variable parameters of the deriving buoyancy force such as permeability and density contrast) is less than some critical value, the fluid remains motionless and heat is transferred by conduction only. The non-horizontal isotherms are able to make fluids flow, without taking into account if the Rayleigh number is less or higher than its critical value. This so-called non-Rayleigh convection is characterized by very slow fluid flow velocities, compared to Rayleigh convection.

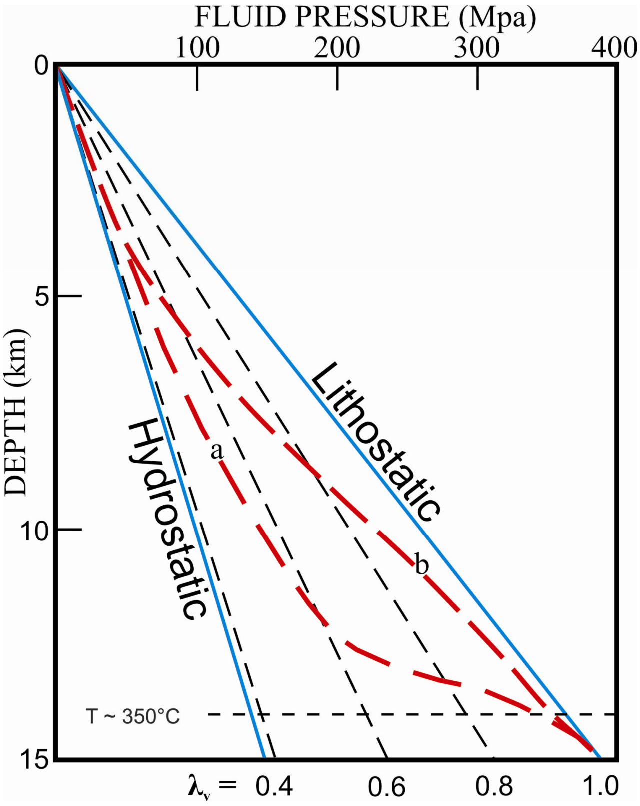

Figure (II.7): Hypothetical fluid pressure profiles, red dashed lines (a,b) represent two progressions from hydrostatic to near lithostatic fluid pressures (modified after Sibson, 2001).

2.2.1 Rayleigh Number

The dimensionless Rayleigh number (Ra) represents the ratio of the buoyant forces and the viscous forces, inhibiting fluid flow (Kühn et al, 2006). Turcotte and Schubert (2002) show linear stability analysis in a fluid saturated porous layer heated from below yields the dimensionless Rayleigh number:

$$Ra = \alpha_f g \rho^2{}_f Cp_f Kz \frac{(T - T_0)}{(\mu\lambda)} \qquad \text{(II.21)}$$

Where subscript f = fluid which is equivalent to water for our case, (T-T_0) is the temperature difference and g is the gravity ($m.s^{-1}$). The critical value of the Rayleigh number Ra_{cr} marks the onset of convection. If $Ra < Ra_{cr}$, disturbances will decay with time; if $Ra > Ra_{cr}$, perturbations will grow exponentially with time. The critical Rayleigh number is a function of the wavelength of the disturbance. Figure (II.8) shows how Ra_{cr} depends on $2\pi z/\lambda$ where b is the depth. If the Rayleigh number and wavelength lie in the zone above the curve, the convection dominates; if the point lies below the curve, convection cannot occur.

In the case shown in figure (II.8), the value of wavelength corresponding to the critical Rayleigh number is:

$$\lambda = 2*(2)^{1/2}*z, \text{ hence } \min(Ra_{cr}) = 4\pi^2 = 39.4784 \qquad \text{(II.22)}$$

Therefore buoyancy forces can be strong enough to overcome the viscous resistance, (Turcotte and Schubert, 2002).

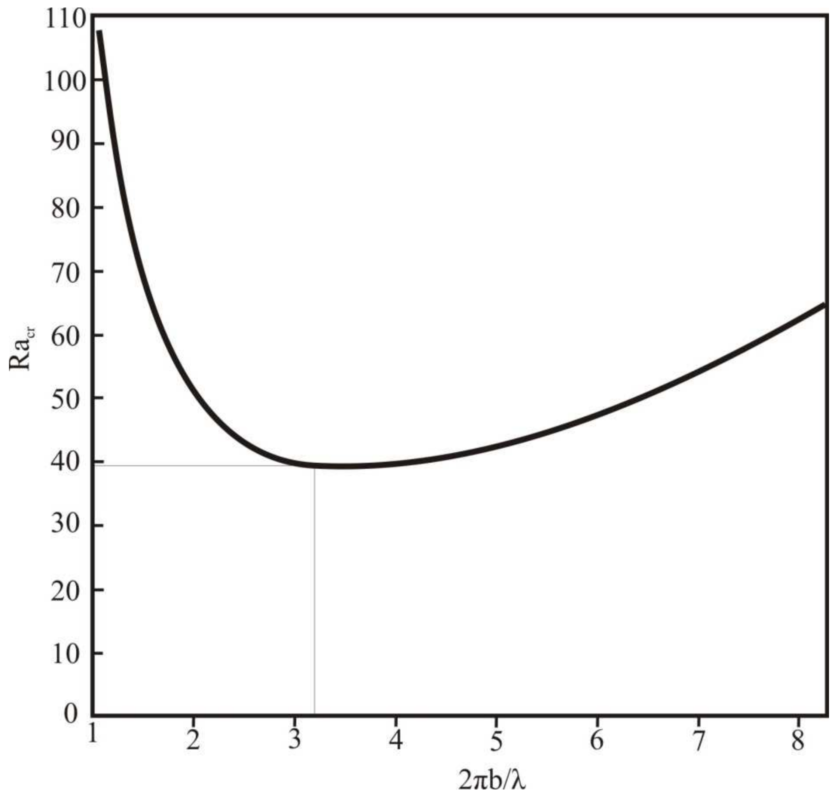

Figure(II.8): critical Rayleigh Number for the onset of convection in a layer of porous material heated from below as a function of dimensionless wave number 2Πz/λ ***(****modified after Turcotte and Schubert, 2002****).***

2.2.2 Peclet Number

The Péclet number is a dimensionless measure of the mean velocity of flow and comparing advection versus diffusion. Pe number can be written as:

$$Pe = u\, R/\kappa \qquad \text{(II.23)}$$

Where u is the velocity vector, R is a characteristic length in (m) and κ is the thermal diffusivity.

To estimate the zone of thermal advection, we have used the Peclet number which is defined as a ratio between advection and thermal diffusion. In fact, Peclet number *Pe* derived from the measured maximum velocities. Thus, when the Peclet number is small, the influence of heat advection is small because of the slow velocity. Therefore, we can say that the vertical velocity increases as the Peclet number increases and the vice versa. There is a critical Peclet number above which the heat advection becomes efficient (Alduncin, 1993; Friedhelm & Igel 1999; Holzbecher, 2005), this critical value is (*Pe)* >1, indicative of the dominance of advection over diffusion.

2.2.3 Heat Transfer

Heat transfer involves two parts, temperature, and heat flow, where heat flow characterizes the movement of thermal energy. On a microscopic scale, thermal energy is related to the kinetic energy of molecules. It is natural for regions of high thermal energy to transfer this energy to regions with less thermal energy (∇T). Physical properties of the medium help or avoid the transferring of thermal energy two regions at differing temperatures. Some of these physical properties are thermal conductivities, specific heats, material densities, fluid velocities, fluid viscosities, and more.

From both laboratory and theoretical studies, the rheology of mantle rocks (as they are treated as semi-viscous or semi-solid in behavior) is partly related to the temperature as a function of depth. Therefore, it is important to know the way in which heat can be lost from the interior to the surface. There are three mechanisms for the transfer of heat: conduction, convection and radiation.

2.2.3.1 Conduction

Heat transfer by conduction is performed by vibrating atoms in any material. The rate at which heat is conducted over time from a unit surface area, called the heat flux or heat flow, is the product of the thermal gradient and the thermal conductivity, or

*Heat flow = thermal conductivity * thermal gradient*

$(W*m^{-2}) \qquad (W*m^{-1}*K^{-1}) \qquad (K*m^{-1})$

The governing equation to express the conductive heat transport is Fourier's law:

$$q = -\lambda * \left(\frac{\partial T}{\partial z} \right) \tag{II.24}$$

Where λ is the coefficient of thermal conductivity and z is the coordinate in direction of the temperature variation. The minus sign is to explain that heat flows in the direction of decreasing temperature, (Best, 2001).

2.2.3.2 Convection

Convection is a movement caused by a density contrast which is a consequence of temperature differences; where less dense material moves upward and more dense moves downward. Convection includes advection, in which mass or heat is transported by the currents or motion in the fluid.

2.2.3.3 Advection

A good example of advection is transport of plate tectonics to a subduction zone, the motion of the heat mantle carries the plate down to the mantle. Another common advected substance is heat, and here fluids may be water, air, or any other heat-containing fluid material. Any substance or conserved property (such as heat) can be advected, and treated mathematically as a scalar concentration of substance and the fluid as a vector field.

2.2.3.4 Radiation

It represents the transfer of electromagnetic energy from the surface of a hot body into the surrounding zone. An example of this way of transfer is the heat transferred from a hot lava into the atmosphere. In a vacuum, this energy moves at 299,800 km/s.

2.2.3.5 Production

We deal with radiogenic heat production which comes from radioactive decay as a specific value for each type of rock or lithological formation as showed in the table below. Heat production is an important way as many types of granite in Australia localized ore deposits cause of high heat production, (McLaren et al., 1999).

Granite	**9.3**
peridotite	**0.020**
Average continental upper crust	**3.9**
Alkali basalt	**1.9**

Table (II.1): Radiogenic heating per mass of some rock types in (10^{-10} $W*kg^{-1}$), (after Fowler, 2001).

2.3 Free convection in numerical view

2.3.1 Heat Transfer

The main equation which calculates temperature in the thermal part includes the convection and conduction heat transfer is expressed as:

$$C_{eq}\left(\frac{\partial T}{\partial t}\right) + \nabla\left[-\lambda_{eq}\nabla T + C_L\vec{u}T\right] = Q \qquad \text{(II.25)}$$

Where C_{eq} denotes the effective volumetric heat capacity; λ_{eq} defines the effective thermal conductivity; and C_L is the volumetric heat capacity of the moving fluid. The total fluid velocity $\vec{u}$ is a vector of directional velocities u, v and w in case of model 3D. The terms on the right hand of the equation Q denote general heat sources in conservative form. We defined C_{eq} and λ_{eq} with equations we have provided about the volume fraction θ, density ρ, specific heat capacity C_p, and thermal conductivity **λ** that varies with temperature. The equations used to define C_{eq} and λ_{eq} are:

$$C_{eq} = (\sum \theta_{Li}\rho_{Li}C_p Li + \sum \theta_{Pi}\rho_{Pi}C_p Pi) \Big/ (\sum \theta_{Li} + \sum \theta_{Pi}) \quad \text{(II.26)}$$

$$\lambda_{eq} = (\sum \theta_{Li}K_{Li} + \sum \theta_{Pi}K_{Pi}) \Big/ (\sum \theta_{Li} + \sum \theta_{Pi}) \quad \text{(II.27)}$$

Here the subscripts $_{\boldsymbol{L}}$ and $_{\boldsymbol{P}}$ denote liquid and solid properties respectively.

2.3.2 Fluid Flow

The Navier-Stokes, Brinkman Richards and Darcy's law equations were done to describe free flows within a river; well, high and low-velocity flows in porous media.

2.3.2.1 Navier-Stokes equation

The Navier-Stokes equations characterize the flow of freely moving fluids. This suits assessments involving liquids and gases that migrate within rivers, pipes, fractures, and streams.

2.3.2.2 Richard's equation

The Richards' Equation analyzes flow in variably saturated porous media. With variably saturated flow, hydraulic properties change as fluids move through the medium, filling some pores and draining others.

2.3.2.3 Brinkman equation

The Brinkman equations describe fast moving fluids in porous media with the kinetic potential from fluid velocity, pressure, and gravity to drive the flow. These equations extend Darcy's law to describe the dissipation of the kinetic energy by viscous shear as with the Navier-Stokes equation. Consequently, this well suits transitions between slow flow in porous media governed by Darcy's law and fast flow in channels described by the Navier-Stokes equations.

2.3.2.4 Darcy's Law

The Darcy's law describes fluid movement through interstices in a porous medium. Fluid losing considerable energy to frictional resistance within pores, the velocities in porous media are very low. However, Darcy's law applies to describe water moving in an aquifer or stream bank, oil migrating to a well, and even magma rising through the earth to a chamber in a volcano.

Darcy's law was applied, when what derives fluid movement in the porous medium is the gradient in hydraulic potential. According to Darcy's law, the net flux across a face of porous surface is:

$$u = \frac{-K}{\mu}(\nabla P + \rho_f g \nabla z) \qquad \text{(II.28)}$$

Where u is the Darcy velocity, K is the permeability of the porous media, μ is the fluid's dynamic viscosity, ρ_f is the fluid's density and P is its pressure, g is the magnitude of gravitational acceleration, and z is the depth in m.

Continuity of generalized governing Darcy's Law is expressed by:

$$S.\partial P \big/ \partial t + \nabla\left[\frac{-K}{\mu}(\nabla P + \rho_f g \nabla z)\right] = Q_s \qquad \text{(II.29)}$$

Where K is the permeability, S is the storage term and Q_s is the strength of a fluid source.

3. Model Setup

Prior to running any numerical model one requires initial and boundary conditions and governing equations. Although, numerical models of the hydrothermal circulations are based upon the same set of governing equations, described here in non-mathematical terms. Numerical methods differ in how the equations are solved; what approximations and assumptions are made and how one represents the physical processes in the physical parameters.

3.1 Model Construction

To construct a numerical model permits to investigate hypotheses concerning mineralization, and can be used in order to guide future mineral exploration, we selected parameters that affect in heat transfer and fluid flow to be varied based on incorporate of a wide range of experimental, natural, analogue, and theoretical data. These parameters are mentioned above followed by the second step is the simplification procedures.

3.1.1 Numerical Simplification

Most numerical studies simulate free convection in 2D only, because fluid patterns are more easily recognised with less complicated geometries, less computational time is required, or computer codes may be restricted to two dimensions. However, geometric complexity and stratigraphic heterogeneity around some ore deposits make it impossible to derive such an exact analytical solution for these systems. In numerical solutions, the simplicity of geometries which represent heterogeneous material properties is necessary for two raisons: 1) the complexity of geometries makes computation time sometimes too long, 2) that the complexity doesn't allow us to test different hypothesises by adding some new geometries to the geological setting; this simplicity doesn't mean ignoring the variabilities of physical parameters which created by the lithological heterogeneity. Based on this principle, we can illustrate the interaction between fluid flow mechanisms and complex geometries and taking into account heterogeneous material properties.

Furthermore, pure water is appropriate for thermal fluid physical properties because meteoric and magmatic waters are composed mainly by pure water (XH_2O between 0.75 to 0.95 at P-T conditions between 1000-4000 bar and 720-930°C) based on data from experimental constraints on volatile abundances in arc felsic magma (Scaillet and Pichavant, 2003). They showed that the fluid compositions of different natural examples of granitic magma were mainly composed by water. Therefore, we have chosen pure water parameters (thermal conductivity, heat capacity, density and viscosity) to represent the physical parameter for fluid in our numerical models.

Finally, initial fluid pore pressure conditions are defined to be hydrostatic using Eq.(19). The porosity in the entire model is set to be constant regardless of the rock type or varying permeabilities. This simplification was done, because a lecture survey of different systems showed that the influence of changing porosity on the flow field is negligible (Kühn et al., 2006).

3.1.2 Parameters and numerical procedures

The initial permeability in the model has been adopted from the studies of Ingebritsen and Manning, (2003). Permeability varies with depth using Eq.(18) in the host rock. In contrast, it has homogeneous and isotropic distributions within the permeable zone (such as faults and fractured aureole).

Flow and heat transport are coupled in the way that the fluid parameters are functions of temperature (Eqs, 1, 2, 3, 7, 8, 10, 15 and 17), while pressure and permeability are varied with depth (Eqs. 18 and 19), all of them updated in the following time step. Therefore, the strength of coupling depends, in principle, on the time step size. As a consequence, sufficiently small time steps are required, and the numerical code adapts the time steps until a convergence criterion is validated. Thermal effects may induce buoyancy driven free convection.

Our coupling is done by incorporation between two parts; the first one is heat transfer and the second one is fluid flow. Our thermal models and coupled models incorporate simple temperature-dependent fluid viscosity, heat capacity, conductivity and density relationships (figure II.9).

Furthermore, in the fluid flow part, we vary the permeability and fluid pressure with depth and adding the viscosity and density which already vary with temperature in the thermal part (heat transfer). This allows the models to recalculate temperature, viscosity, density, heat capacity, thermal conductivity, fluid pressure and permeability at every time-step in solver parameters. Based on these variable data every time-step we obtain a new output which becomes input for the next time-step.

The models were made in 2D except the model of Tighza pluton (the main natural example) which has been made in 3D. However, simpler models (i.e. thermal) have been tested extensively in the past and are routinely compared to results from field measurements.

3.1.3 Models Classification

One hundred ninety two models were carried out to examine three objectives mentioned above. Models of first scenario are divided into three types according to the objectives.

1. Numerous of models were made to verify the heat transfer and fluid flow coupling.
2. The first type (seventy seven models) includes simple geometry for intruded magma (square, tabular, rectangular and vertical magma bodies) within a host rock, and different hypotheses such as emplacing of different intrusions at the same or different depth at the same or different times. The physical properties of magma are represented in our simulations as granitic magma body, while host rock represents here a general metamorphic rock (mica-schist) by using the physical parameters of metamorphic rocks. These models were done to examine the first goal and to be as a data base and reference when we compare them with other models (Figure II.10).
3. The second type is to distinguish the role of apexes on the same system and the distribution of ore deposits around intrusion body. Thirty three models were created with different number and size of apexes; we keep the depth and the time of emplacement constant as they were tested in the first type.
4. In the third type, we attempted to simulate nineteen models to study the role of permeable zone (such as faults and fracture systems) which are derived from natural examples
   - a- Ten models were made, to test the effect of permeable zone as a large fault nearby the magma chamber; we varied here the values of permeability for the permeable zone; the values of permeability were 10^{-14}, 10^{-15} and $10^{-16}m^2$.
   - b- Nine models were to test the effect of fracture systems on the distribution of heat and fluid circulation around intruded magma and inside permeable zone. The same values of permeability for the large fault were kept as in the pervious class (the difference between fractured zone around pluton and large faults is that faults were active with permeability $10^{-15}m^2$ the whole computational time, while the fractured zone was activated only between 9.5 to 12Myr)

Other secondary models were added to validate our models (seven models) and study the different natural examples (thirty four models), which are divided into two major parts.

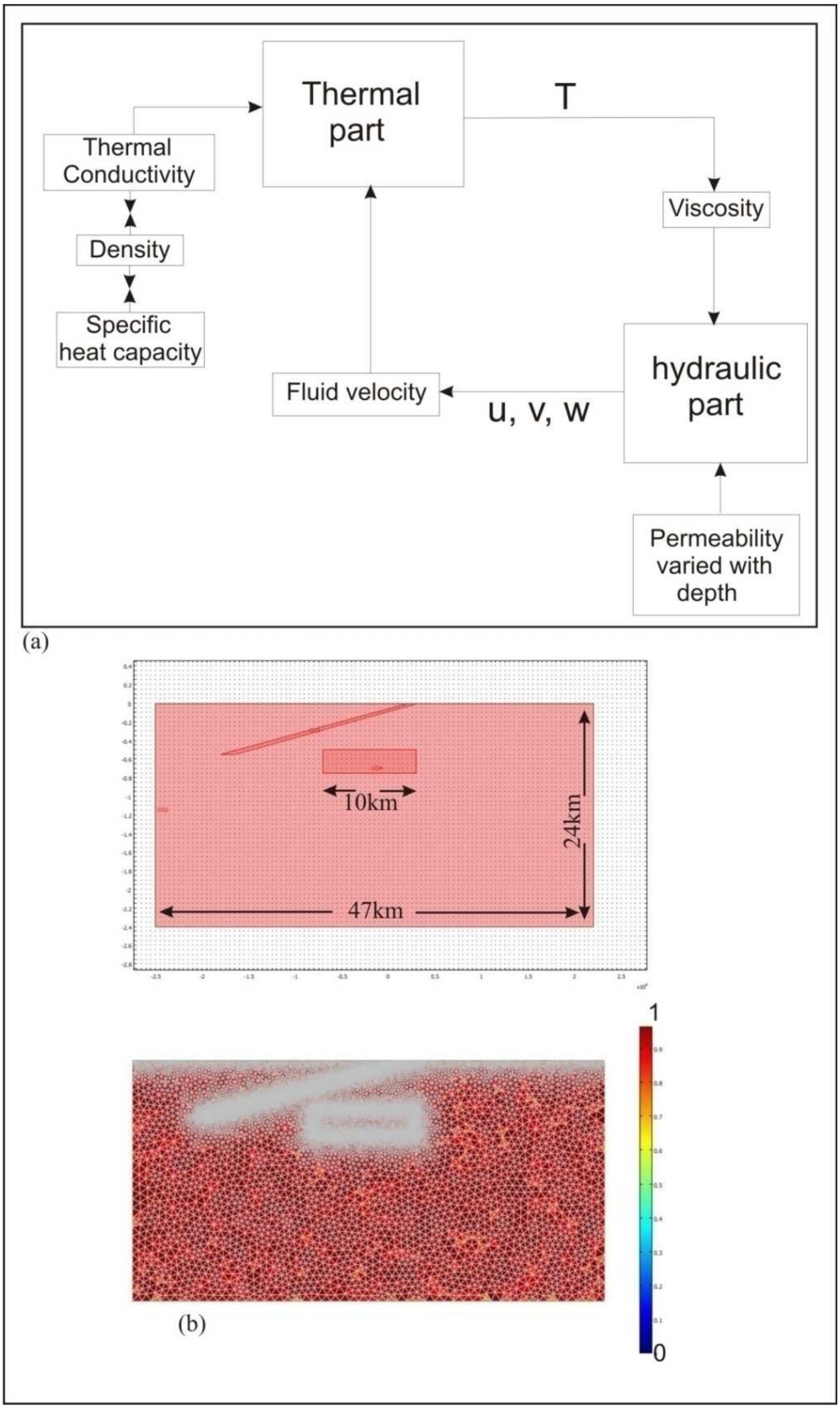

Figure (II.9) (a) Schematic digram of our hydrothermal numerical coupling, (b) an example of our models shows the quality of mesh elements (the minimum value is 0.7/1), the grey zone around the fault and intrusion represents refine mesh elements ($5*10^{-8}$ m) for the accuracy (in zones where parameters vary faster than in other zones), convergence and speed of the solution.

3.1.3.1 The first part (Theoretical and natural cases)

The models of this scenario were made to discuss the effects of depth of emplacement, emplacement of one or more pluton at the same or different time, geometry of pluton, large permeable faults and fracture systems and the role of apexes. Three domains were created, (1) A host rock with a permeability varied with depth by using Eq.(18), the geometry of host rock is fixed for all our models, with 47 km width and 24 km depth, the porosity is constant here (5%) as its influence on the flow field in negligible (Kühn et al., 2006).

Physical properties (such as thermal conductivity, heat capacity, density and viscosity) are varied by using equations (II.1, II.2, II.4, II.7, II.8, II.10, II.15 and II.17) based on data representing physical properties of metamorphic and igneous rocks, (2) intruded hot body in these models type is also fixed dimensionally (10 km width and 2.5 km length).

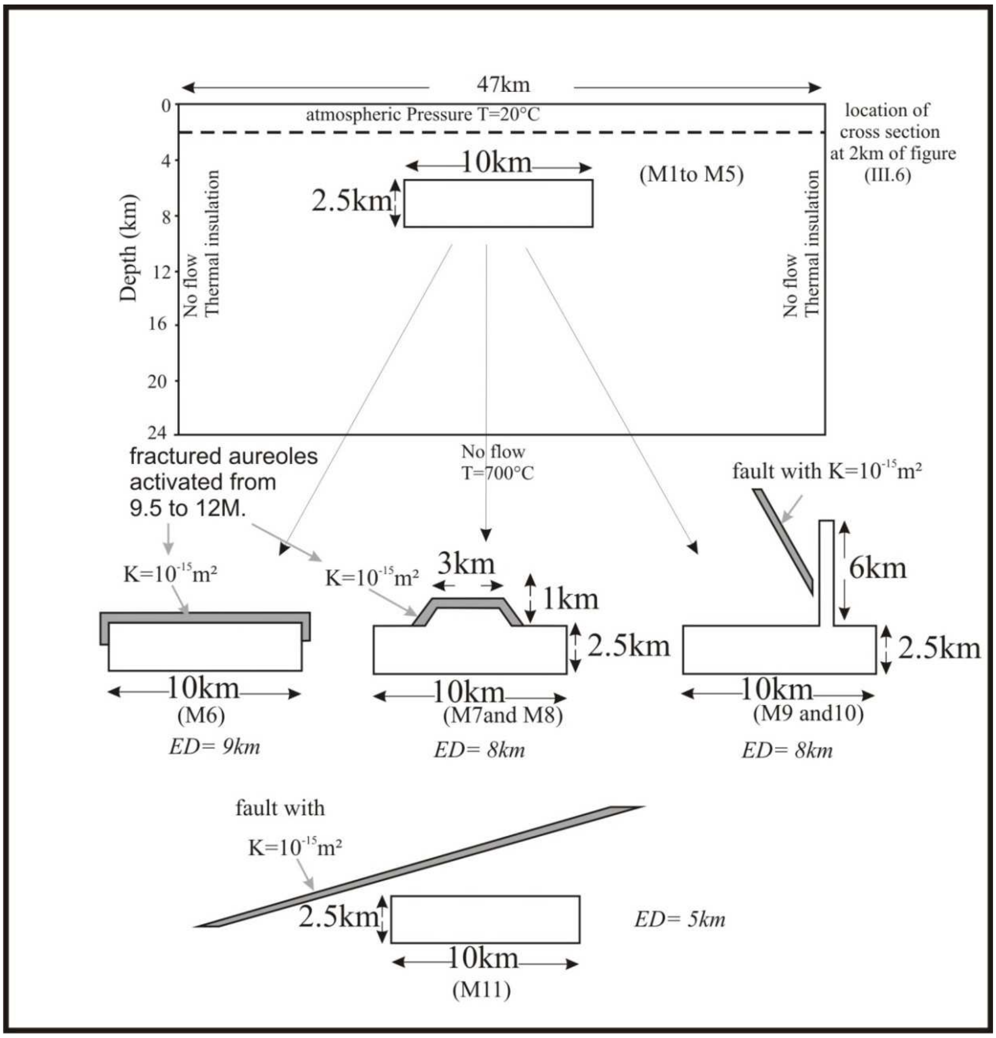

Figure (II.10): Boundary and initial conditions of our numerical models, with different forms of intruded magma. M1 to M11 correspond theoretical and natural examples mentioned in chapter (III), ED is emplacement depth.

The hot intruded body emplaced during 3 Myrs. and produces radiogenic heat 9.3 10^{-10} W/kg. We consider our pluton as a compacted crystalline granitic body by using granite physical parameters with constant porosity (5%), (3) in some cases, we added permeable systems such as fault and/or fracture, the permeability of these zones were varied between 10^{-14}, 10^{-15} and 10^{-16}m². Other hypothesis were made by changing the form of pluton by adding dykes or apexes with or without permeable fault (see below for details).

3.1.3.2 The second part (Tighza example)

In this part, we introduce a 3D geometry of pluton, and create a numerical model with real geometry. This example comes from Hercynian natural case (Tighza Pluton, central Morocco), where the mineralization related pluton is presented.

The 3D geometry of this pluton was constrained by gravity measurements, and made by using a software presented in chapter (IV) where we will discuss in detail the natural example and the processing to obtain the geometry of pluton.

3.2 Validation and applications

In order to make sure the computational results of a particular numerical model is reliable and consistent with the flow physics under investigation, capabilities of this numerical model for predicting realistic physical processes and phenomena have to be confirmed before the model is accepted and applied to simulating real world problems. A numerical model is a complex system of equations wrapped with boundary conditions, it is not guaranteed to have these capabilities even it has been proven to be mathematically correct, unless they have been validated with physical model data or with a model that was already published.

In addition, a numerical model for general flow simulation should have many validation tests using different physical models (natural examples and/or published numerical models) should be carried out to evaluate each one of them.

The test cases selected in this research are divided into two types, natural and published types. The natural models selected are four natural examples; they will be described in detail in next chapter, while the selected published numerical models are represented by two models done by (Rabinowicz et al., 1998 ; Gerdes et al., 1998).

3.2.1 The first validation test (Rabinowicz model)

This example explains the hydrothermal convection within a sedimentary layer in the Middle Valley which is a sedimented rift valley in the northern Juan de Fuca Ridge. Rabinowicz et al; (1998) have constructed their model by using the following initial conditions: (a) the equations are solved in a rectangular domain of (3 to 5.5 km). (b) No flow passes through the bottom of the box, and the dimensionless temperature along this interface is kept constant and equal to 400°C. (c) Along the top of the box, the dimensionless temperature is equal to 0, and the fluid is free to enter and leave the simulation domain. (d) Pressure is constant along the top interface. (e) They also varied viscosity, density and pressure with temperature and depth respectively by inserting physical laws, while heat capacity and thermal conductivity were inserted to the model as constant values. (f) The governing equations were Darcy's law and heat transfer equations.

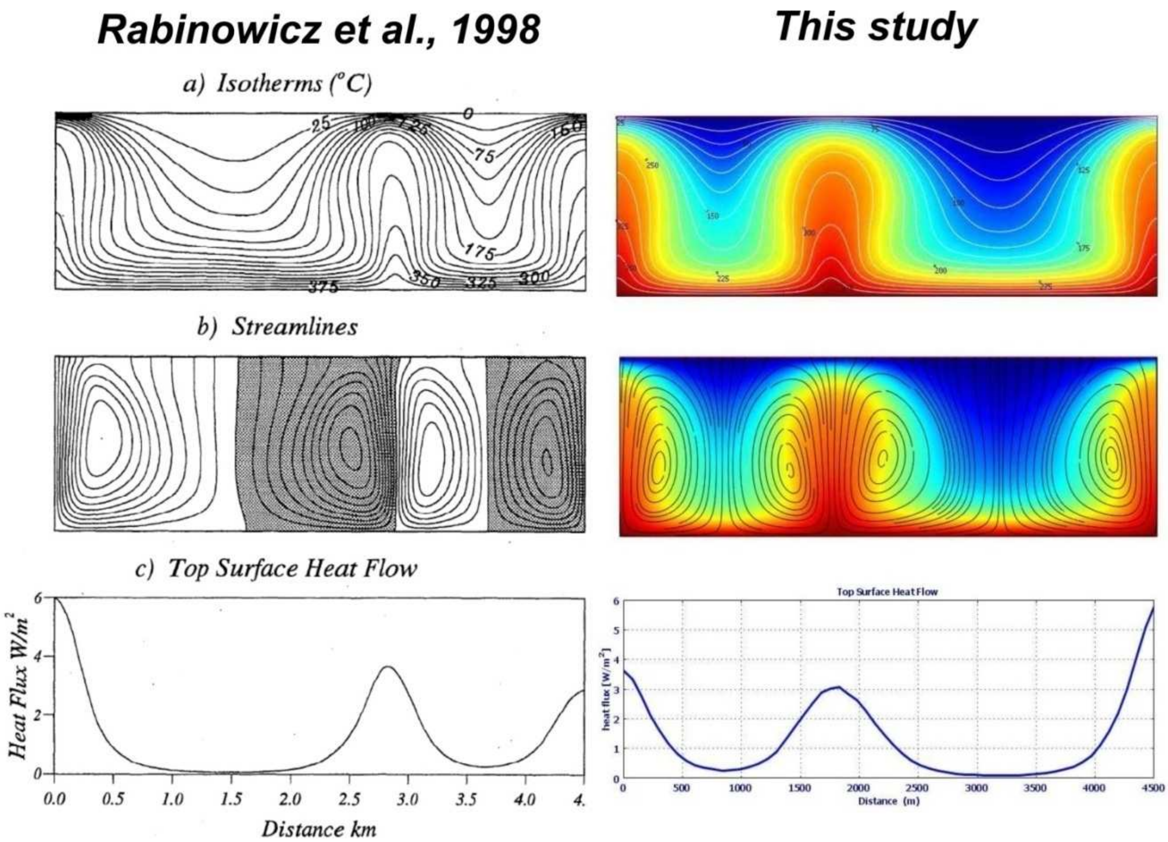

Fig.(II.11) Rabinowicz model (in the left side) and the equivalent test made by our numerical coupling (in the right side).

Figure (II.11) shows their model and the equivalent model made by us based on their available initial conditions. May you have noted the slight difference between the two models in heat flux, we referred this to their boundary condition at the base which was not well detailed. Therefore, we increased the temperature at the bottom to reach 400°C. During time, convective pattern adapts and gets a similar unsteady behavior as the one described by Rabinowicz et al. (1998).

3.2.2 The second validation test (Gerdes Model)

Gerdes et al. (1998) have used stochastic representations of permeability in a series of transient numerical simulations to assess how much small-scale rock heterogeneities influence kilometer-scale fluid convection around a shallow crustal pluton. They consider different permeability values by varying statistical characteristics of the permeability distribution.

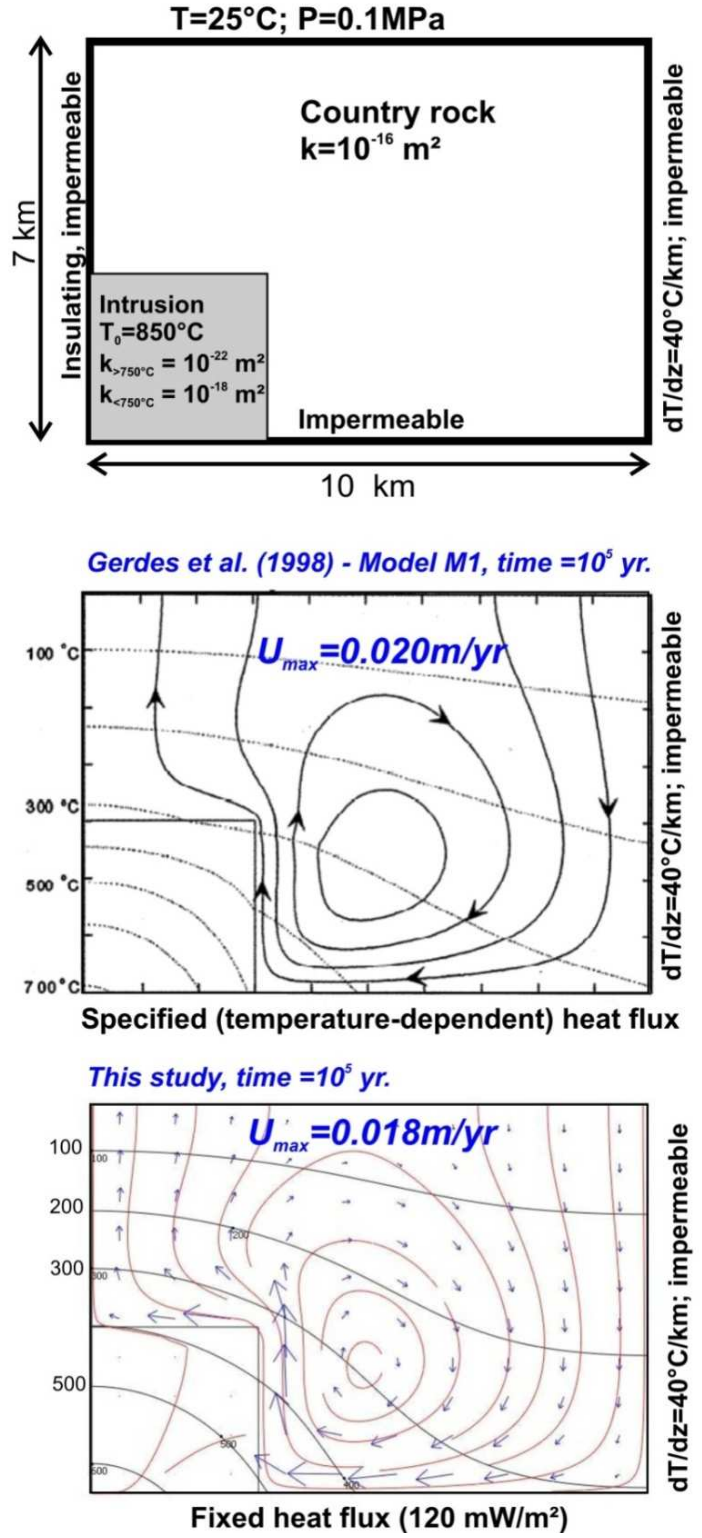

Figure (II.12) An identical model of (Gerdes et al (1998) at the middle) reproduced by our numerical coupling (at the bottom).

They have used the mass conservation equation and Darcy's law as governing equations for fluid flow, while the conservation of energy equation includes both conductive and advective heat transport. Figure (II.12) shows our simulation of their simplest model, where permeability is constant in the host rock. A negligible difference in measured fluid velocity was noted ($0.002m*yr^{-1}$), and convective patterns are almost identical, we referred the slight difference in streamlines to their boundary condition at the bottom which were not clear.The next chapter represents our work on different natural example and our discussion of different essential questions.